J Mol Med (2005) 83: 377–385
DOI 10.1007/s00109-004-0629-x

ORIGINAL ARTICLE

Jasmina Lovrić · Hassan S. Bazzi · Yan Cuie · Genevieve R. A. Fortin · Françoise M. Winnik · Dusica Maysinger

Differences in subcellular distribution and toxicity of green and red emitting CdTe quantum dots

Received: 30 July 2004 / Accepted: 30 November 2004 / Published online: 2 February 2005

Abstract Quantum dots (QDs) are emerging as alternative or complementary tools to the organic fluorescent dyes currently used in bioimaging. QDs hold several advantages over conventional fluorescent dyes including greater phototability and a wider range of excitation/emission wavelengths. However, recent work suggests that QDs exert deleterious effects on cellular processes. This study examined the subcellular localization and toxicity of cadmium telluride (CdTe) QDs and pharmacological means of preventing QD-induced cell death. The localization of CdTe QDs was found to depend upon QD size. CdTe QDs exhibited marked cytotoxicity in PC12 and N9 cells at concentrations as low as 10 μg/ml in chronic treatment paradigms. QD-induced cell death was characterized by chromatin condensation and membrane blebbing and was more pronounced with small ($2r$=2.2±0.1 nm), green emitting positively charged QDs than large ($2r$=5.2±0.1 nm), equally charged red emitting QDs. Pretreatment of cells with the antioxidant *N*-acetylcysteine and with bovine serum albumin, but not Trolox, significantly reduced the QD-induced cell death. These findings suggest that the size of QDs contributes to their subcellular distribution and that drugs can alter QD-induced cytotoxicity.

Keywords Quantum dots · Fluorescence · Toxicity · Cell death · Antioxidants

J. Lovrić · G. R. A. Fortin · D. Maysinger (✉)
Department of Pharmacology and Therapeutics,
McGill University, McIntyre Medical Sciences Building,
3655 Promenade Sir-William-Osler,
Montreal, QC, H3G 1Y6, Canada
e-mail: dusica.maysinger@mcgill.ca
Tel.: +1-514-3981264
Fax: +1-514-3986690

H. S. Bazzi · Y. Cuie · F. M. Winnik
Faculty of Pharmacy and Department of Chemistry
Universite de Montreal, Pavillon J.A. Bombardier,
C.P. 6128 Succursale Centre-Ville,
Montreal, QC, H3C 3J7, Canada

JASMINA LOVRIĆ received her B.Sc. degree in pharmacy at University of Zagreb, Croatia. She is presently completing the experimental part of her Ph.D. thesis at McGill University, Montreal, Canada. Her project focuses on quantum dots as novel tools in bioimaging and nanoparticles as drug delivery systems.

DUSICA MAYSINGER earned her Ph.D. degree at the University of Southern California, Los Angeles, USA and had postdoctoral training at the Max Planck Institute in Munich, Germany, Karolinska Institut in Stockholm, Sweden, and Oxford University, UK. She is now Associate Professor at McGill University, Montreal, Canada. Research in her laboratory focuses on investigating therapeutic interventions in diabetes and neurodegenerative disorders in conjunction with nanodelivery systems and the effectiveness of drugs from the nanodelivery systems in modulating signal transduction pathways in cell death and differentiation.

Abbreviations *BSA*: Bovine serum albumin · *CdSe*: Cadmium selenide · *CdTe*: Cadmium telluride · *DAF*: 5-Dodecanoylaminofluorescein · *MPA*: Mercaptopropionic acid · *MTT*: 3-(4,5-Dimethylthiazol-2-yl)-2, 5-diphenyl tetrazolium bromide · *NAC*: *N*-Acetylcysteine · *PBS*: Phosphate-buffered saline · *QD*: Quantum dot

Introduction

Quantum dots (QDs) are semiconductor inorganic nanoparticles that are emerging as alternative or complementary tools to the organic fluorescent dyes currently used in bioimaging. In comparison with traditional organic fluorophores, QDs have a number of advantages including broad excitation and narrow emission spectra [1–3] which allow the simultaneous resolution of multiple colored probes using a single light source. In addition, QDs are more resistant to photobleaching than their organic counterparts, thus making the long-term labeling and monitoring of live cells more feasible.

QDs have traditionally been prepared in organic solvents [4, 5], and their resulting hydrophobic character rendered them unsuitable for use in biological systems due to a marked loss of fluorescence in aqueous media [1]. Water-soluble QDs that retain strong fluorescence can now be prepared by exchange of the organic capping layer with a hydrophilic moiety such as an acid functionalized thiol [2, 6, 7]. However, the preparation of such QDs is a difficult procedure, and direct preparation methods for water-soluble QDs have paved the way for their increased use in biological applications [8]. We employed the latter method for the preparation of cadmium telluride (CdTe) QDs in this study.

Although QDs have great potential as probes for bioimaging [9–13], certain limitations may restrict their usefulness. Due to their particulate nature QDs tend to aggregate, especially in the presence of serum proteins. In addition, QD fluorescence is susceptible to quenching in the biological milieu. The potential toxicity of QDs is a growing concern in spite of early studies in immortalized cell lines that showed little or no deleterious effects of QDs in chronic treatment paradigms [1, 14–16]. A more recent study using primary cultures of hepatocytes revealed a concentration-dependent toxicity of cadmium selenide (CdSe) QDs at concentrations above 0.0625 mg/ml under certain conditions such as oxidation or exposure to ultraviolet light [17]. QD-induced toxicity was found to be correlated with the liberation of free cadmium ions (Cd^{2+}), and surface coatings such as ZnS, polyacrylate [16], and dihydrolipoic acid [15] that reduce QD surface oxidation and subsequent release of free Cd^{2+} were shown to improve biocompatibility. The potential toxicity of other types of QDs, including CdTe QDs, has not previously been investigated.

The aim of this study was to examine the subcellular localization and toxicity of CdTe QDs and to explore pharmacological means of preventing QD-induced cell death. We provide evidence that the size of QDs is a major determinant of their subcellular distribution and toxicity.

Materials and methods

Preparation of anionic QDs

$NaBH_4$(0.8 g, 21.15 mmol) was dissolved in water (20 ml) at 0°C. Tellurium powder (1.28 g, 10.03 mmol) was added portion-wise, and the mixture was stirred at 0°C under N_2 for 8 h, yielding a purple solution. The reaction mixture was kept at 4°C in the dark and used in the next step. Cd $(ClO_4)_2$ (0.25 ml, 1 M aqueous solution) and 3-mercaptopropionic acid (MPA; 0.2 g, 1.884 mmol) were dissolved in water (200 ml). The pH of the solution was adjusted to 10.5 using 1 M KOH prior to addition of NaHTe solution (0.1 ml). The reaction mixture became light brown in color and was heated to reflux. Aliquots were taken as the reaction proceeded, and the fluorescence spectra were recorded to monitor the QDs growth as a function of reaction time. A green emission (λ_{em}=530 nm) was observed after 15 min. The maximum emission wavelength shifted to longer wavelengths as the reaction proceeded. After 7.5 h the mixture was cooled to room temperature and kept in the dark prior to further modification.

Preparation of cationic QDs

Anionic QDs (20 ml) were dialyzed against deionized water for 18 h with frequent changing of the water. Dialysis was performed using spectra/por membrane tubing (Spectrum Laboratories) with a 6–8 kDa molecular weight cutoff. Aggregates formed and were collected by centrifugation at 14,000 rpm with an Eppendorf 5415C centrifuge. The pellet was washed with MeOH and air-dried. The resulting solid (15 mg) was dispersed in cysteamine hydrochloride (20 ml, 0.24% aqueous solution). The resulting solution was sonicated for 2 h in a Branson 1210 sonicating bath, forming a clear solution which was kept in the dark until use. Dynamic light scattering measurements of anionic and cationic QDs were performed on a CGS-3 ALV instrument (Langen, Germany), and zeta potentials were measured using a ZetaPlus Analyzer (Brookhaven Instruments, Holtsville, N.Y., USA).

Synthesis of QD-BSA conjugates

Anionic QDs (λ_{em}=692 nm, 3.75 mg) were dissolved in phosphate-buffered saline (PBS, 0.5 ml), and the resulting solution was mixed with a solution of bovine serum albumin BSA (Sigma, Oakville, Ont., Canada; 0.5 ml, 10 g/l in PBS). A freshly prepared solution of 1-[3-(dimethylamino)propyl]-3-ethyl-carbodiimide hydrochloride (0.05 M, 0.1 ml) was then added, and the resulting solution was stirred at room temperature for 2 h. The solution was then purified by dialysis against PBS to remove free BSA. UV-Vis: λ_{max}=214 nm, 228 nm, 286 nm, and 310 nm; λ_{em}=693 nm.

Measurement of QD fluorescence

Fluorescence spectra were recorded using a Cary Eclipse Fluorescence spectrometer (Palo Alto, Calif., USA; excitation wavelength=400 nm, excitation/emission slits were set at 5 nm). The fluorescence quantum yields (Φ) of the QDs were calculated by comparing their integrated fluorescence intensities with those of rhodamine 6G in water. The QD solutions were diluted in PBS (pH 7.2), and the absorbance of the solutions was between 0.02 and 0.03. The following equation was used: $\Phi_s=(I_s/I_r)\times(A_r/A_s)\times\Phi_r$, where I_s and I_r are the integrated fluorescence intensities between 425 and 790 nm of the sample and the reference, respectively, A_r and A_s are the absorbances at 400 nm of the reference and the sample, respectively, and Φ_r is the quantum yield of rhodamine 6G in water (0.98) [18].

Cell culture conditions

Rat pheochromocytoma cells (PC12) (American Type Culture Collection, Rockville, Md., USA), were maintained at 37°C (5% CO_2) in RPMI 1640 medium containing 5% fetal bovine serum (Gibco, Burlington, Ont., Canada). The N9 murine microglial cell line was generously provided by Philippe Séguéla (Montreal Neurological Institute, Montreal, Que., Canada). N9 cells were maintained in Iscove's modified Dulbecco's media containing 5% fetal bovine serum. All media were free of phenol-red and contained 1% penicillin-streptomycin. For spectrofluorometry and colorimetric assays cells were seeded in 24-well plates (Sarstedt, Montreal, Que., Canada) at a density of 10^5cells/cm^2.

Cell treatments

Two hours prior to treatments cells were washed, and media was replaced with either serum-containing or serum-free media, as indicated. For toxicity studies cationic QDs were added to cells at concentrations between 0.01 and 100 μg/ml for 24 h. *N*-Acetylcysteine (NAC; Sigma) was used at a final concentration of 2 mM and added to cells either (a) concomitantly with QD addition, (b) for 2 h and then removed before QD addition, or (c) for 2 h prior to QD addition and maintained continuously in the media. Trolox (Sigma) and BSA (Sigma) were used at final concentrations of 1 mM and 2.5 mg/ml (38 μM), respectively, and were added to the cells for 2 h prior to QD addition (maintained continuously in the media).

Assessment of cell metabolic activity

Colorimetric 3-(4,5-dimethylthiazol-2-yl)-2,5-diphenyl tetrazolium bromide (MTT) assays were performed to assess the metabolic activity of cells treated as described above. After 24-h treatment medium was removed and replaced by drug-free, serum-free media (500 μl/well). To each well 50 μl stock MTT (5 mg/ml) was added, and cells were then incubated for 1 h at 37°C. Medium was removed, and cells were lysed with dimethylsulfoxide (Sigma). Absorbance was measured at 595 nm using a Benchmark microplate reader (Bio-Rad, Mississauga, Ont., Canada).

Confocal microscopy and assessment of cell nuclei size

Microscopy was performed using a confocal laser scanning LSM 510 Zeiss microscope equipped with following lasers: (a) HeNe LASOS LGK 7786 P/power supply 7460 A: 543 nm 1 mW, (b) argon LASOS LGK 7812 ML-1lGN: 458, 488, 514 nm 25 mW, laser class 3D, and (c) titanium: sapphire Coherent Mira Model 900-F laser tunable from 710 to 1000 nm for two photon microscopy (set to pulse at 800 nm). Cells were seeded into eight-well chambers (Lab-Tek, Nalge Nunc International, Rochester, N.Y., USA) at density of 10^5 cells/cm^2. QDs were added to designated wells, and the cells were incubated for different time periods from 5 min to 24 h. Plasma membranes were labeled with 5-dodecanoylaminofluorescein (DAF; 1 μM, Molecular Probes, Eugene, Ore., USA) and nuclei were labeled with Hoechst 33342 (10 μM, Molecular Probes). Cells were washed once with PBS or acidified wash (0.5 M NaCl, 0.2 M CH_3COOH, pH 2.5), once with PBS, and then once with serum-free medium to remove any nonspecifically adsorbed QDs or any free fluorescent dye. No background cell fluorescence was detected under the settings used. Nuclear sizes were analyzed using Scion Image software (Frederick, Md., USA), and figures were created using Adobe Photoshop.

QD uptake assay

A Molecular Devices SpectraMax Gemini XS microplate spectrofluorometer was used for quantitative measurements of fluorescence of cells incubated in the presence of QDs and respective controls. Total fluorescence was measured at the end of the incubation periods. Cells were then washed once with acidified wash (10 s) or PBS, then once more with PBS and lysed with dimethylsulfoxide. The amount of fluorophore in the cells was calculated as the ratio of fluorescence from cell lysates after acidified

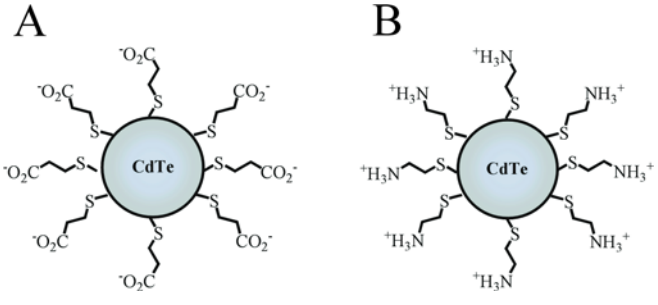

Fig. 1 Schematic presentation of negatively (**A**) and positively (**B**) charged CdTe quantum dots

Table 1 Physicochemical properties of quantum dots

Quantum dots	λ_{em} (nm)[a]	Φ[b]	ζ-potential (mV)	Diameter (nm, ±0.1)
Anionic green	530	0.05	−38.60	2.3
Cationic green	535	0.01	+22.10	2.2
Anionic red	632	0.05	−41.75	5.7
Cationic red	640	0.01	+20.68	5.2

[a]Emission maximum
[b]Quantum yield

washing to the total fluorescence. The excitation wavelength was 400 nm for all QDs, and the emission maxima were 640 nm for red cationic QDs and 535 nm for green cationic QDs.

Statistical analysis

Data were analyzed using Systat 10 (SPSS, Chicago, Ill., USA). Statistical significance was determined by analysis of variance followed by Tukey's post hoc test. Differences were considered significant at $P<0.05$.

Results

Preparation and characterization of QDs

Negatively charged water-born QDs (Fig. 1A) were prepared following the general procedure previously reported by Gao et al. [8] using MPA as a stabilizer. QDs grew in size as the reaction proceeded, and consequently their emission underwent a shift to a longer wavelength (Table 1). Green-emitting QDs ($2r$=2.3 nm, λ_{em}=530 nm) were formed after 15 min, while red-emitting QDs were generated after 7.5 h ($2r$=5.7 nm, λ_{em}=630 nm). The QD solutions were stored in the dark at 4°C and were stable for at least 4 months, as determined by measuring their size and emission properties. The resulting QDs were anionic (ζ-potential=-41.75 mV) and their fluorescence quantum yields were 0.05 (relative to rhodamine 6G in PBS) [18].

Cationic QDs were generated by the exchange of the MPA stabilizing layer of the anionic QDs with a cysteamine hydrochloride layer (Fig. 1B). This treatment was carried out by first removing MPA from the QD surface by dialysis, resulting in neutral nanoparticles that were purified by repeated centrifugations. QDs were then dispersed in an aqueous solution of cysteamine hydrochloride. The success of the stabilizer exchange was confirmed by ζ-potential measurement (Table 1). The emission wavelengths of the positive QDs were similar to those of the respective negative QDs, but the quantum yields were significantly reduced. This decrease in the fluorescence quantum yield of the positive QDs relative to the negative QDs might be due to differences in the packing efficiency of the positively and negatively charged stabilizers. The size of the QDs was not affected by the stabilizer exchange.

BSA was covalently linked to anionic QDs by reaction of the carboxylic groups on their surface with the amine groups of the protein using 1-[3-(dimethylamino)propyl]-3-ethyl-carbodiimide hydrochloride as a coupling agent [1, 19]. Sodium dodecyl sulfate polyacrylamide gel electrophoresis confirmed that BSA was covalently linked to the QDs in a ratio of 1:1 (data not shown). CdTe QDs have been previously conjugated to BSA, and it was also found that they predominantly form 1:1 BSA:CdTe conjugates with a minor component of 2:1 BSA:CdTe conjugates [20].

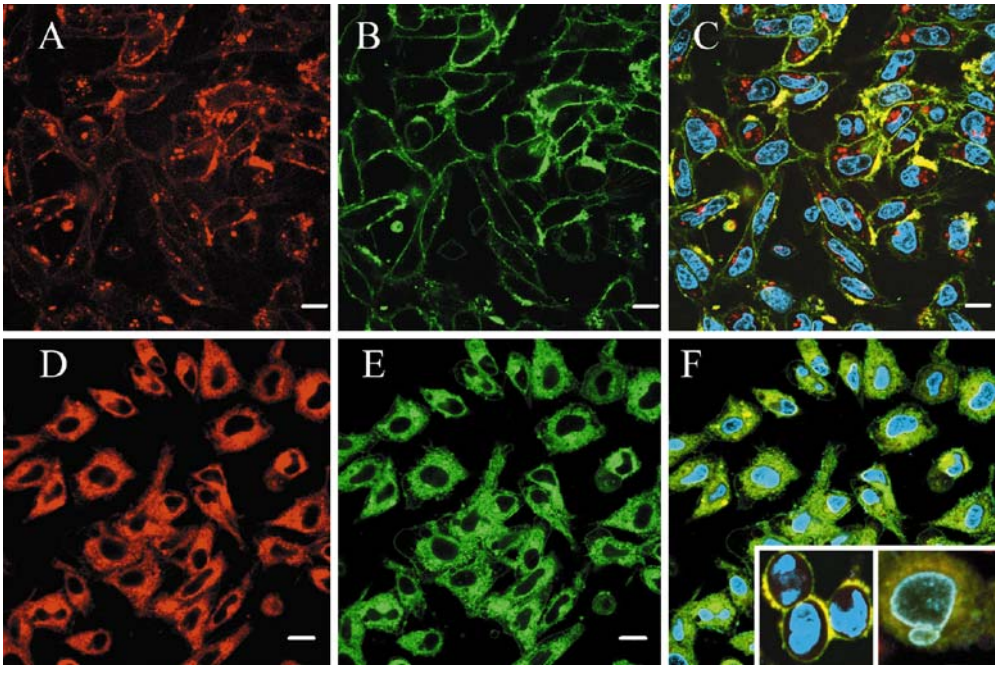

Fig. 2 Confocal micrographs of PC12 cells treated with positively charged, red QDs. **A**–**C** PC12 cells were incubated with red cationic QD (3.75 µg/ml) for 5 min (**A**), with DAF (1 µM) for 1 min (**B**), or Hoechst (10 µM) for 1 h and the obtained images were superimposed (**C**). **D**–**F** PC12 cells incubated with high concentration of QDs (37.5 µg/ml) for 5 min (**D**), with DAF (1 µM) for 1 min (**E**), Hoechst (10 µM) for 1 h and the obtained images were superimposed (**F**). *Scale bar* 10 µm. *Inserts* show rounding of cells and nuclear blebbing after 1 h treatment with QDs (37.5 µg/ml)

Morphological changes in PC12 cells exposed to CdTe QDs

To assess the subcellular distribution of CdTe QDs we treated PC12 cells with either low (3.75 μg/ml) or high (37.5 μg/ml) concentrations of red cationic QDs. PC12 cells treated with low concentrations of red cationic QDs showed some punctuate distribution in the cytoplasm (Fig. 2A) but were not detected in the nucleus (Fig. 2C). Colocalization of red QDs with the cell membrane was revealed by staining with the membrane specific green fluorescent dye (DAF; Fig. 2B, C). Confocal microscopy and spectrofluorometry of red QD-treated cells subsequently subjected to acidified washing indicated that the association of QDs with the cell membrane was loose and nonspecific, being almost completely removed by the washing (approx. 85% reduction in total fluorescence; data not shown). We have evidence that QD fluorescence has not been extinguished by acidified washing of cells. Confocal microscopy using cells washed only with PBS or washed with acidified wash for 10 s followed by immediate washing with PBS resulted in comparable intracellular distributions of QDs. Moreover, we measured the fluorescence intensities of QDs in media (pH range from 3–10) and found that the acidification of the media can enhance the fluorescence. The fluorescence intensity was maximal at pH 5.5, and it was decreased by either raising or lowering the pH.

High concentrations of red QDs showed a widespread cytoplasmic distribution but were not detected within the cell nuclei (Fig. 2D-F). After 1 h of exposure to high-dose QDs cell rounding (Fig. 2F, left insert), chromatin condensation, and nuclear membrane blebbing (Fig. 2F, right insert) became apparent, indicative of cell toxicity. After 24 h of incubation with a high concentration of red QDs 50% of cells displayed condensed nuclear morphology (nuclear diameter <10 μm; data not shown).

Metabolic activity of PC12 and N9 cells treated with CdTe QDs

Based on the observed changes in cell morphology we proceeded to investigate QD-induced toxicity in a chronic exposure paradigm at concentrations above and below those optimal for confocal microscopy. Metabolic assessments were conducted in both serum-free media (to avoid interference of QDs with serum components) and serum-containing media, which more closely mimics in vivo conditions. At concentrations optimal for confocal imaging (1–10 μg/ml) neither red cationic nor green cationic CdTe QDs induced significant changes in metabolic activity in PC12 cells within the time interval required for such studies (30–60 min, data not shown). After 24 h of exposure, higher QD concentrations (10–100 μg/ml) caused a significant decrease in cell metabolic activity ($P<0.05$; Fig. 3A, B). In addition, green QDs were significantly more toxic than red QDs at the highest concentration tested in PC12 cells (100 μg/ml) (Fig. 3A, B, decrease in metabolic activity: 68.8±1.4% and 46.8±2.3%, respectively, $P<0.05$). In N9 cells green and red QDs also exerted toxic effects after 24 h (Fig. 4A, decrease in metabolic activity: 66.6±2.3% and 46.5±1.2%, respectively; $P<0.05$). In addition, the presence of serum in the media significantly protected both N9 cells (Fig. 4A; $P<0.05$) and PC12 cells (data not shown) exposed to both types of QDs.

Subcellular localization of red and green cationic QDs

The difference in the toxicity caused by CdTe QDs of different sizes prompted us to examine the subcellular localization of red vs. green cationic QDs. The most striking difference in QD localization as revealed by confocal microscopy was observed in the nuclear vs. cytoplasmic compartments. Red QDs were distributed throughout the cytoplasm of N9 cells but did not enter the nucleus within

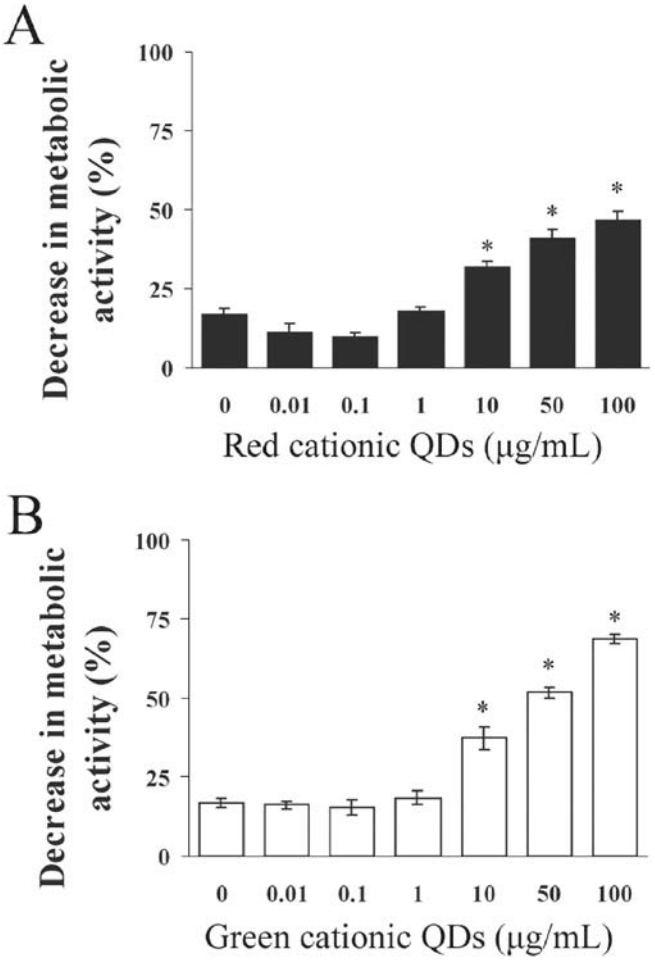

Fig. 3 Metabolic activity of PC12 cells treated with CdTe QDs. PC12 cells were exposed to red and green cationic QDs in the concentration range of 0.01–100 μg/ml for 24 h in serum-free media, after which time metabolic activity was assessed by MTT assay. Data are expressed as proportional decrease in metabolic activity relative to the control values from cells to which no QDs were added and which were grown in serum-containing media. *Columns* Group means ±SEM for triplicate samples from three or four independent experiments. *$P<0.05$

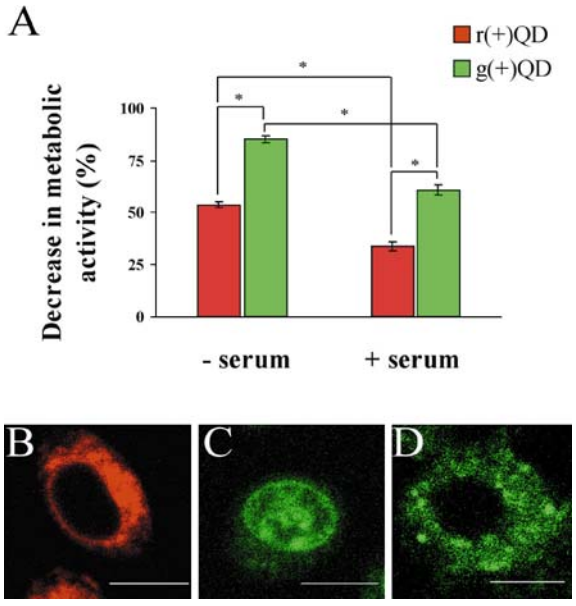

Fig. 4 Differential toxicity and subcellular localization of red and green cationic QDs. **A** N9 cells were exposed to red [*r(+)QD*, 7.5 μg/ml] and green [*g(+)QD*, 7.5 μg/ml] cationic QDs in serum-free and serum-containing media for 24 h. Ordinate represents decrease in metabolic activity relative to controls not treated with QDs. *Columns* Group means ±SEM for quadruplicate samples from three or four independent experiments. *$P<0.05$. **B** Red cationic QDs (3.75 μg/ml, 1 h incubation) are distributed within the cytoplasmic compartment of N9 cells. **C** Green cationic QDs (1.25 μg/ml, 1 h incubation) were localized mostly in the nucleus of N9 cells. **D** Green QD-BSA complex (1 h incubation) revels the fluorescent signal mainly in the cytosol. *Scale bar* 10 μm

1 h (Fig. 4B). In contrast, green QDs were localized predominantly in the nuclear compartment within the same time frame (Fig. 4C). However, green QDs bound to BSA were mainly seen in the cytosol (Fig. 4D).

Effect of antioxidants in PC12 cells exposed to red cationic QDs

Previous studies have demonstrated that antioxidants can protect against Cd^{2+}-induced cell death [21–23]. We investigated whether QD-induced cell toxicity can be prevented by free radical scavengers such as NAC and Trolox. When NAC was added to PC12 cells for 2 h prior to QD addition and maintained in the medium, the QD-induced reduction in cell metabolic activity was completely prevented (Fig. 5A; $P<0.05$). Simultaneous addition of NAC with QDs afforded a lesser degree of protection against cell death (79.1±1.7%). NAC pretreatment alone without continued presence of NAC in the medium failed to protect the cells against QD-induced cytotoxicity. Trolox was found to be ineffective in preventing the QD-induced decrease in cell metabolic activity at the concentrations tested (Fig. 5B; $P>0.05$).

Effect of conjugated and nonconjugated BSA on QD-induced cytotoxicity

Previous studies have shown that conjugation of BSA to the surface of MPA-coated, ZnS-capped CdSe QDs can significantly decrease QD-induced toxicity [17]. We therefore investigated the potential protective effects of BSA against CdTe QD-induced changes in metabolic activity. Both nonconjugated BSA and BSA conjugated to nega-

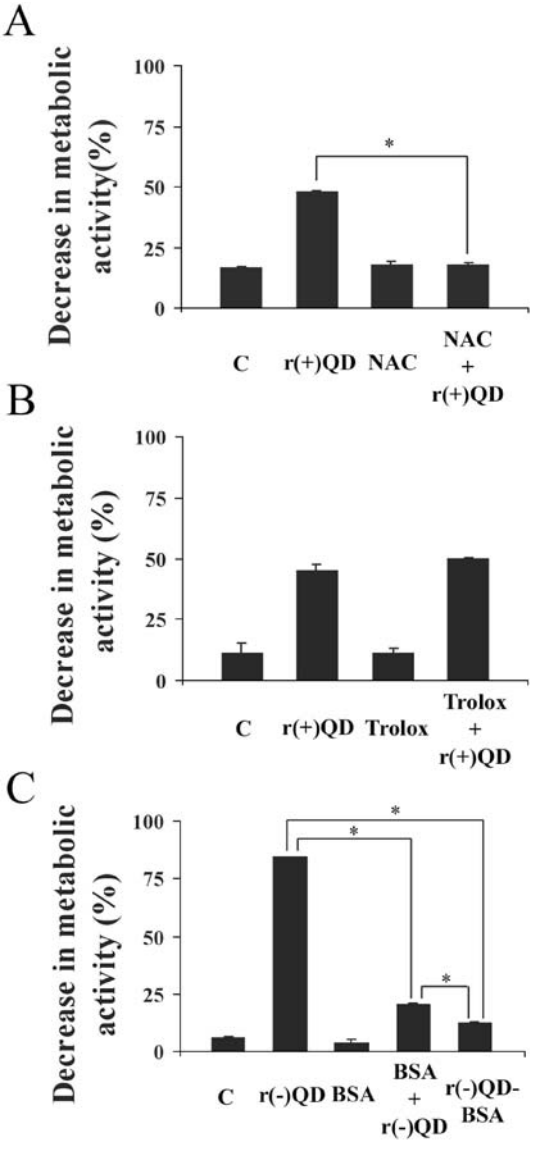

Fig. 5 Metabolic activity of QD-treated PC12 cells exposed to NAC, Trolox, and BSA. The data are expressed as proportional decrease in metabolic activity relative to the control values from cells to which no QDs were added, and which were grown in serum-containing media. **A** Protective effect of NAC (2 mM) after 24 h exposure to red cationic QD [*r(+)QD*, 50 μg/ml] in the continuous presence of the drug. **B** Trolox treatment (1 mM) is ineffective in rescuing cells from QD toxicity (red cationic, 50 μg/ml). **C** Protective effect of BSA (2.5 mg/ml, 38 μM) or BSA conjugated to red anionic QD [*r(−)QD*] in the equivalent concentrations of red anionic QDs. *Columns* Group means ±SEM for quadruplicate samples from three or four independent experiments. *$P<0.05$

tively charged QDs provided protection against cytotoxicity in PC12 cells (Fig. 5C), with greater protective effects afforded by the BSA when conjugated to QDs (Fig. 5C; $P<0.05$).

Discussion

In the present study we demonstrate that: (a) CdTe QDs can enter the cell and distribute in different subcellular compartments; (b) CdTe quantum dots exert cytotoxicity characterized by changes in cell nuclear morphology as well as by decreases in the metabolic activity; (c) QD-induced toxicity can be reduced by NAC, BSA, or the presence of serum proteins in the medium, and (d) the mechanism of QD-induced cytotoxicity may be mediated by mechanisms other than free radical formation.

As previously reported for CdSe QDs [15], we found that CdTe QDs enter the cell. After a short time of incubation CdTe QDs are visible at the cell surface and in the cytoplasm. QDs likely bind to the cell surface due to the interaction with cell surface glycoproteins and glycolipids [14]. Employing red- and green-emitting cationic QDs in our experiments, we found that the CdTe QD distribution was in part dependent on nanoparticle size. In the murine microglial N9 cell line red cationic QDs ($2r$=5.2 nm) were distributed throughout the cytoplasm (Fig. 4B). In contrast, green also positively charged QDs ($2r$=2.2 nm) were often found in the nucleus of N9 cells upon 1 h of QD exposure (Fig. 4C). Bruchez et al. [13] have shown that green QDs coated with tri-metoxysilylprolyl urea and acetate groups bind with high affinity in the cell nucleus of mouse 3T3 fibroblasts. In human mammary epithelial tumor cells (MDA-MB-231) green-emitting CdSe/ZnS/SiO_2 QDs were packaged in large vesicles found in the perinuclear region [14]. In contrast to the findings by Parak et al. [14] that the size of the nanocrystals does not influence the intake and distribution of QDs, our data provide evidence that CdTe QDs induce cytotoxicity which is partly dependent on the size of the nanoparticles. Since relatively unrestrained passage of macromolecules up to 9 nm in diameter occurs through nuclear pores [24], the size of the individual QDs ($2r$=2.2–5.2 nm) cannot be the only explanation for the entry of smaller green QDs into the nucleus. There are several possibilities. CdTe QDs as well as the other uncoated QDs, often form aggregates in the biological medium. We observed that green QDs stay in the medium as a clear, stable colloid system for more than 1 month whereas the red QDs often precipitate. Even if the green QDs form small aggregates consisting of two or three particles, they would still be able to enter the nucleus. In contrast, the same number of red QDs would be too large to cross the nuclear membrane. The other possibility is that QDs could form complexes with cell proteins. In the case of green QDs the formed complex may enter the nucleus or may be too unstable to retain the green QDs in the cytosol. On the other hand, red QDs complexed with cytosolic proteins are too large to enter the nucleus.

Upon the exposure of cells to high QD concentrations (>30 μg/ml) cells begin to change their morphology. After 1 h of incubation with QDs nuclear membrane blebbing and cell rounding was easily detected (Fig. 2F, inserts).

Previous work by Derfus et al. [17] suggests that cytotoxicity of QDs is correlated with the concentration of Cd^{2+} liberated as a result of the deterioration in CdSe lattice. In the present study Cd^{2+} could have been released from the CdTe QDs and in similar manner contributed to the observed toxicity. Nevertheless, the significant difference between the toxicity induced by red and green positively charged QDs suggests the involvement of other mechanisms of QD-induced cell death. It is conceivable that green cationic QDs, due to their significantly smaller size, can more readily enter the cell, the nucleus, and possibly other subcellular compartments, thereby causing the more pronounced cytotoxicity. The QD-induced changes in cell morphology may shed further light on the cause of cell death. Upon chronic treatment of PC12 cells with red cationic QDs, approx.50% of the cells underwent nuclear condensation and displayed pycnotic nuclei ($2r$<10 μm), while the remaining cells presented normal nuclear morphology. These cell death mechanisms may be due to the presence of free Cd^{2+}, the formation of free radicals, or the interaction of nanoparticles with individual cellular components leading to their malfunction and ultimately to cell death. The concentrations of CdTe QDs used in our study are in the same range as those used in several other studies. For example, Shiohara et al. [25] recently showed that mercaptoundecanoic acid–CdSe QDs cause a decrease in the metabolic activity of several different cell types at QD concentrations of 50 μg/ml or higher. Toxicity was concentration and cell type dependent. However, we employed smaller concentrations of QDs than those used in the work by Jaiswal et al. [15] and Derfus et al. [17]. In the Jaiswal et al. studies, after uptake of dihydrolipoic acid capped ZnS/CdSe QDs, HeLa cells were labeled for over 1 week with no detectable changes on cell morphology or physiology. In the studies by Derfus et al. mercaptoacetic acid–CdSe QDs in the concentration range of 0.0625–1 mg/ml did not significantly reduce the metabolic activity of hepatocytes as assessed by MTT. Commercial, protein-conjugated QDs are larger than uncoated, unconjugated CdTe or CdSe QDs and are reported to be nontoxic in the 20- to 40-nmol concentrations [16].

We hypothesized that the QD-induced toxicity was a consequence of free radical generation and thus tested the effects of antioxidants NAC and Trolox on cellular damage (Fig. 5). Interestingly, these two antioxidants exerted completely different effects. Millimolar concentrations of NAC were effective at reducing QD-induced cytotoxicity, whereas Trolox, the water soluble analog of vitamin E failed to prevent cell death under the same conditions. α-Tocopherol can reduce oxidative stress in biological membranes. It reacts with a lipid peroxyl radical thereby acting as a lipophilic chain breaking agent [26, 27]. The failure of Trolox to reduce QD-induced toxicity suggests that free radicals are not the exclusive contributors to the QD-

induced cell death. The effectiveness of NAC could be explained by at least three mechanisms of action: (a) NAC contains a mercapto group that could allow it to be adsorbed to the surface of QDs and thus stabilize the QDs in culture media; (b) its protective activity can be attributed to its antioxidant properties and its ability to enhance glutathione expression [28]; (c) NAC can activate key antiapoptotic signal transduction pathways that lead to transcription of genes involved in cell survival [29, 30].

Previous findings that the conjugation of BSA to CdSe QDs reduces QD-induced toxicity [17] were also observed in this study with CdTe QDs. Albumin represents an important component of the extracellular antioxidant defense system, and one of the possible explanations for the high scavenging efficiency of BSA is the large proportion of tyrosine and tryptophane [31]. Tyrosinyl and tryptophanyl peptides may be unique biological moieties to be attached to QDs to possibly reduce or eliminate their toxicity.

The reduction in QD toxicity by BSA pretreatment or conjugation of BSA to QDs could be due to differences in the subcellular localization of unmodified and modified QDs. We have prepared and tested both complexes of and conjugates of QDs with BSA and assessed the distribution of these QDs by confocal microscopy. In contrast to the small, unmodified QDs, those bound to BSA were localized mainly in the cytosol (Fig. 4D). Similar studies have been reported by Hanaki et al. [32], who demonstrated that QD–albumin complexes can be considered as photostable endosomal markers.

The cytoprotection afforded by both NAC and BSA suggests that the QD-induced toxicity is partially induced by Cd^{2+}. One of the mechanisms of Cd^{2+} toxicity is its binding to sulfhydryl groups of mitochondrial proteins [33], and NAC has been shown to be a powerful inhibitor of Cd^{2+}induced cell death [34]. Moreover, BSA is well known for its metal-binding sites with which it can complex cadmium ions [35] and prevent cytotoxicity.

In summary, our studies show that the physicochemical characteristics of CdTe QDs influence their subcellular localization and their cytotoxicity. Our findings suggest that QD-induced cytotoxicity is in part dependent on QD size and is characterized by chromatin condensation and membrane blebbing. In addition, QD-induced cytotoxicity is significantly reduced by treatment of cells with NAC or BSA. Moreover, BSA QDs conjugates are significantly less toxic than free QDs, supporting previous observations with CdSe QDs [17]. It therefore appears that although native QDs may be cytotoxic, they can become innocuous towards cells by the addition of pharmacological agents that do not otherwise affect the cellular mechanisms under scrutiny.

Acknowledgements This work was supported by the Juvenile Diabetes Research Foundation (Canada) and NanoQuebec. We thank Dr. E. Kumacheva (Department of Chemistry, University of Toronto) for helpful discussions and for suggestions on the preparation of water soluble QDs. J.L. also thanks J. Tam and R. Aikin for useful discussion and stylistic revisions of the manuscript.

References

1. Chan WC, Nie S (1998) Quantum dot bioconjugates for ultrasensitive nonisotopic detection. Science 281:2016–2018
2. Chan WC, Maxwell DJ, Gao X, Bailey RE, Han M, Nie S (2002) Luminescent quantum dots for multiplexed biological detection and imaging. Curr Opin Biotechnol 13:40–46
3. Jovin TM (2003) Quantum dots finally come of age. Nat Biotechnol 21:32–33
4. Mattoussi H, Mauro JM, Goldman ER, Anderson GP, Sundar VC, Mikulec FV, Bawendi MG (2000) Self-assembly of CdSe-ZnS quantum dot bioconjugates using an engineered recombinant protein. J Am Chem Soc 122:12142–12150
5. Dabbousi BO, Rodriguez-Viejo J, Mikulec FV, Heine JR, Mattoussi H, Ober R, Jensen KF, Bawendu MG (1997) (CdSe) ZnS core shell quantum dots: synthesis and characterization of a size series of highly luminescent nanocrystallites. J Phys Chem B 101:9463–9475
6. Pathak S, Choi SK, Arnheim N, Thompson ME (2001) Hydroxylated quantum dots as luminescent probes for in situ hybridization. J Am Chem Soc 123:4103–4104
7. Wuister SF, Swart I, van Driel F, Hickey SG, Donega CD (2003) Highly luminescent water-soluble CdTe quantum dots. Nano Lett 3:503–507
8. Gao M, Kirstein S, Mvhwald H, Rogach AL, Kornovski A, Eyhmiller A, Weller Horst (1998) Strongly photoluminescent CdTe nanocrystals by proper surface modification. J Phys Chem B 102:8360–8363
9. Lidke DS, Nagy P, Heintzmann R, rndt-Jovin DJ, Post JN, Grecco HE, Jares-Erijman EA, Jovin TM (2004) Quantum dot ligands provide new insights into erbB/HER receptor-mediated signal transduction. Nat Biotechnol 22:198–203
10. Dahan M, Levi S, Luccardini C, Rostaing P, Riveau B, Triller A (2003) Diffusion dynamics of glycine receptors revealed by single-quantum dot tracking. Science 302:442–445
11. Dubertret B, Skourides P, Norris DJ, Noireaux V, Brivanlou AH, Libchaber A (2002) In vivo imaging of quantum dots encapsulated in phospholipid micelles. Science 298:1759–1762
12. Gao X, Nie S (2003) Molecular profiling of single cells and tissue specimens with quantum dots. Trends Biotechnol 21:371–373
13. Bruchez M Jr, Moronne M, Gin P, Weiss S, Alivisatos AP (1998) Semiconductor nanocrystals as fluorescent biological labels. Science 281:2013–2016
14. Parak WJ, Boudreau R, Le Gros M, Gerion D, Zanchet D, Micheel CM, Williams SC, Alivisatos AP, Larabell C (2002) Cell motility and metastatic potential studies based on quantum dot imaging of phagokinetic tracks. Adv Mater 14:882–885
15. Jaiswal JK, Mattoussi H, Mauro JM, Simon SM (2003) Long-term multiple color imaging of live cells using quantum dot bioconjugates. Nat Biotechnol 21:47–51
16. Wu X, Liu H, Liu J, Haley KN, Treadway JA, Larson JP, Ge N, Peale F, Bruchez MP (2003) Immunofluorescent labeling of cancer marker Her2 and other cellular targets with semiconductor quantum dots. Nat Biotechnol 21:41–46
17. Derfus AM, Chan WCW, Bhatia SN (2004) Probing the cytotoxicity of semiconductor quantum dots. Nano Lett 4:11–18
18. Magde D, Wong R, Seybold PG (2002) Fluorescence quantum yields and their relation to lifetimes of rhodamine 6G and fluorescein in nine solvents: improved absolute standards for quantum yields. Photochem Photobiol 75:327–334
19. Hermanson GT (1996) Bioconjugate techniques. Academic Press, New York
20. Mamedova NN, Kotov NA, Rogach AL, Studer J (2001) Albumin-CdTe nanoparticle bioconjugates: preparation, structure, and interunit energy transfer with antenna effect. Nano Lett 1:281–286
21. Poliandri AH, Cabilla JP, Velardez MO, Bodo CC, Duvilanski BH (2003) Cadmium induces apoptosis in anterior pituitary cells that can be reversed by treatment with antioxidants. Toxicol Appl Pharmacol 190:17–24

22. Almazan G, Liu HN, Khorchid A, Sundararajan S, Martinez-Bermudez AK, Chemtob S (2000) Exposure of developing oligodendrocytes to cadmium causes HSP72 induction, free radical generation, reduction in glutathione levels, and cell death. Free Radic Biol Med 29:858–869
23. Warren S, Patel S, Kapron CM (2000) The effect of vitamin E exposure on cadmium toxicity in mouse embryo cells in vitro. Toxicology 142:119–126
24. Weis K (2003) Regulating access to the genome: nucleocytoplasmic transport throughout the cell cycle. Cell 112:441–451
25. Shiohara A, Hoshino A, Hanaki K, Suzuki K, Yamamoto K (2004) On the cyto-toxicity caused by quantum dots. Microbiol Immunol 48:669–675
26. Sies H, Murphy ME (1991) Role of tocopherols in the protection of biological systems against oxidative damage. J Photochem Photobiol B 8:211–218
27. Bisby RH, Parker AW (1995) Reaction of ascorbate with the alpha-tocopheroxyl radical in micellar and bilayer membrane systems. Arch Biochem Biophys 317:170–178
28. Cotgreave IA (1997) N-Acetylcysteine: pharmacological considerations and experimental and clinical applications. Adv Pharmacol 38:205–227
29. Yan CY, Ferrari G, Greene LA (1995) N-Acetylcysteine-promoted survival of PC12 cells is glutathione-independent but transcription-dependent. J Biol Chem 270:26827–26832
30. Yan CY, Greene LA (1998) Prevention of PC12 cell death by N-acetylcysteine requires activation of the Ras pathway. J Neurosci 18:4042–4049
31. Moosmann B, Behl C (2002) Secretory peptide hormones are biochemical antioxidants: structure-activity relationship. Mol Pharmacol 61:260–268
32. Hanaki K, Momo A, Oku T, Komoto A, Maenosono S, Yamaguchi Y, Yamamoto K (2003) Semiconductor quantum dot/albumin complex is a long-life and highly photostable endosome marker. Biochem Biophys Res Commun 302:496–501
33. Belyaeva EA, Korotkov SM (2003) Mechanism of primary Cd2+-induced rat liver mitochondria dysfunction: discrete modes of Cd2+ action on calcium and thiol-dependent domains. Toxicol Appl Pharmacol 192:56–68
34. Wispriyono B, Matsuoka M, Igisu H, Matsuno K (1998) Protection from cadmium cytotoxicity by N-acetylcysteine in LLC-PK1 cells. J Pharmacol Exp Ther 287:344–351
35. Sadler PJ, Viles JH (1996) H-1 and Cd-113 NMR investigations of Cd2+ and Zn2+ binding sites on serum albumin: competition with Ca2+, Ni2+, Cu2+, and Zn2+. Inorg Chem 35:4490–4496